Articles

Contribution from the Departments of Chemistry and Physics, Kent State University, Kent, Ohio 44242

Long-Lived Chromium(IV) and Chromium(V) Metabolites in the Chromium(VI)–Glutathione Reaction: NMR, ESR, HPLC, and Kinetic Characterization

Rathindra N. Bose,* Shadi Moghaddas, and Edward Gelerinter

Received May 8, 1991

The reduction of Cr(VI) by glutathione (GSH) in an excess of the oxidized form of glutathione (GSSG) proceeds through long-lived intermediates in the pH range 1.8–3.5. Time domain magnetic susceptibility measurements yielded a molar susceptibility of 3.6 ± 0.2 × 10^{-3} cm^3/mol for the intermediates corresponding to a magnetic moment of 2.9 ● 0.1 μ_B at 25 °C for the intermediate. The magnetic moment data along with the ESR measurements unequivocally establish that Cr(IV) is the dominant long-lived intermediate in this reaction and that Cr(V) accounts for <5% of the intermediate. These intermediates are formed by two parallel pathways: an internal electron-transfer process within a Cr(VI)–thioester precursor (k_{et} = 7.2 × 10^{-3} s^{-1}; $K_{formation}$ = 4.0 × 10^2 M^{-1} at pH 2.70) and a bimolecular reaction between the precursor complex and GSH (k = 0.89 M^{-1} s^{-1}). Second-order rate constants increase with the increase in [H^+], consistent with the established acid-catalyzed substitution mechanism for Cr(VI) centers. Conditional formation constants for the thioester complex (evaluated from this study and earlier reports by others) follow a similar trend. This trend in conditional formation constants indicates that the rate of dissociation for the precursor complex does not increase as much as the rate of its formation with an increase in [H^+]. The chromium(IV) intermediate further reacts with GSH to form Cr(III) products. The magnetic susceptibility and magnetic moment for the Cr(III) products were evaluated to be 6.7 ± 0.2 × 10^{-3} cm^3/mol and 4.0 ● 0.1 μ_B. The decomposition of the intermediate is a second-order processes (first with respect to each reactant) (k = 0.13 M^{-1} s^{-1} at pH 2.7), and the second-order rate constants exhibit no appreciable change with the change in pH. Chromium(III) products obtained in GSSG or in self-buffered (GSH) show very similar spectral features: two absorption bands near 570 nm (ϵ = 31–33 M^{-1} cm^{-1}) and 410 nm (ϵ = 26–31 M^{-1} cm^{-1}). It is proposed that rapid ligand exchange or rearrangement takes place prior to the rate-limiting reduction of Cr(IV) by the tripeptide. Major chromium(III) product(s) are monocationic and contain at least 1 mol of GSH and 0.5 mol of GSSG/mol of Cr(III).

Introduction

The carcinogenic/mutagenic activities of chromium(VI) compounds are documented in vivo and in cultured cells.[1,2] Chromium(VI) metabolism by various cellular components is thought to be responsible for such activity since no significant DNA damage is encountered during the interaction of Cr(VI) with isolated DNA.[3] Among the various metabolic pathways, generation of Cr(V) by a variety of "redox active" cellular proteins is a prime suspect. This oxidation state of chromium is a putative DNA-damaging agent and has been shown to be a long-lived intermediate in redox reactions of Cr(VI) with cytoplasmic proteins, cytochrome P-450, and mitochondria.[4-8]

The generation of one or more long-lived Cr(V) intermediates during the redox reaction of Cr(VI) with glutathione (GSH) at neutral pH has been documented by several groups.[9-11] Although

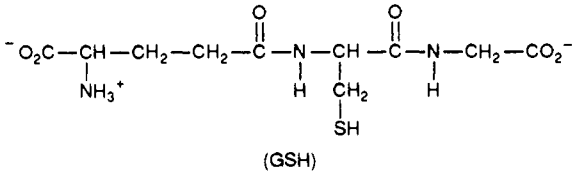

(GSH)

a number of kinetic studies on this redox reaction have already appeared,[12-14] there seems to be little agreement over the detailed mechanism of this reaction. McAuley and Olatunji[12] have reported that this redox reaction is associated with the growth and decay of an absorbing intermediate. On the basis of UV–visible spectroscopic data these workers concluded that the intermediate is a thioester of Cr(VI) (initial step) with a large formation constant (1.4 × 10^3 M^{-1} at 25 °C) followed by subsequent electron transitions (second step) to form Cr(III) and oxidized glutathione products. Electron paramagnetic resonances were observed for intermediates when high concentrations of chromium(VI) along with glutathione were used in flat quartz cells above pH 4. Accordingly, these intermediates are reported to be Cr(V) species.[9-11] Wetterhahn and co-workers[13] particularly emphasized the detailed mechanism of formation of Cr(V) and Cr(IV) intermediates by a number of thiols, on the basis of the evaluation of rate constants by the initial rate method from biphasic rate profiles. These authors suggested that Cr(V) and Cr(IV) intermediates are formed through parallel one- and two-electron reductions and that electron-transfer steps are slower than Cr(VI)–thioester complex formation. A similar mechanism was proposed by Kwong and Pennington[15] for redox reactions involving cysteine and Cr(VI). Recently, O'Brien and Ozolins[14] proposed that the intermediate is a Cr(V) species formed by a rapid disproportionation reaction of Cr(IV). Chromium(IV) is initially formed by a rate-limiting two-electron reduction process. We have documented mechanistic details of redox reactions between Cr(V)

* To whom correspondence should be addressed at the Department of Chemistry, Kent State University.

(1) Sky-Peck, H. H. Trace Metals and Neoplasia. *Clin. Physiol. Biochim.* **1986**, *4*, 99–41. Babich, H.; DeVanas, M. A.; Stotzky, G. *Environ. Res.* **1985**, *37*, 253–286.
(2) Aiyar, J.; Berkovits, H. J.; Floyd, R. A.; Wetterhahn, K. E. *Chem. Res. Toxicol.* **1990**, *3*, 595–603. Rossi, S. C.; Wetterhahn, K. E. *Carcinogenesis* **1989**, *10*, 913–920. Aiyar, J.; Borges, K. M.; Floyd, R. A.; Wetterhahn, K. E. *Toxicol. Environ. Chem.* **1989**, *22*, 135–148 and references therein.
(3) Fan, A. M.; Harding-Barlow, I. *Adv. Mod. Environ. Toxicol.* **1987**, *11*, 87–125.
(4) Kawanishi, S.; Inove, S.; Sand, S. *J. Biol. Chem.* **1986**, *261*, 5952–5958.
(5) Banks, B. R.; Cooke, R. T. *Biochem. Biophys. Res. Commun.* **1986**, *137*, 8–14.
(6) Wetterhahn-Jennette, K. *J. Am. Chem. Soc.* **1982**, *104*, 874.
(7) Rossi, S. C.; Gorman, N.; Wetterhahn, K. E. *Chem. Res. Toxicol.* **1988**, *1*, 101–107.
(8) Ryberg, D.; Alexander, J. *Biochem. Pharmacol.* **1984**, *33*, 2461–2466.
(9) Wetterhahn, K. E.; Cupo, D. Y.; Connett, P. H. *Trace Subst. Environ. Health* **1984**, *18*, 154–162.
(10) Goodgame, D. M. L.; Joy, A. M. *J. Inorg. Biochem.* **1986**, *26*, 219–224.
(11) Kitagawa, S.; Seki, H.; Kametani, F.; Sakurai, H. *Inorg. Chim. Acta* **1988**, *152*, 251–255.
(12) McAuley, A.; Olatunji, M. A. *Can. J. Chem.* **1977**, *55*, 3335–3340.
(13) Connett, P. H.; Wetterhahn, K. E. *J. Am. Chem. Soc.* **1985**, *107*, 4282–4288.
(14) O'Brien, P.; Ozolins, Z. *Inorg. Chim. Acta* **1989**, *161*, 261–266.
(15) Kwong, D. W. J.; Pennington, D. E. *Inorg. Chem.* **1984**, *23*, 2528–2532.

0020-1669/92/1331-1987$03.00/0

and a variety of metal and non-metal reductants utilizing Rocek's chromium(V) complexes[16] in aqueous solution.[17-19] We hoped that some of the known features of Cr(V) redox chemistry might help us understand the rate processes that take place in Cr(VI)–glutathione reaction. Moreover, recently we have outlined a new NMR-based kinetic method to characterize paramagnetic intermediates and products including ESR-silent species.[20] We have applied this method to characterize the intermediates.[21] Moreover, despite several studies on this redox reaction, the fate of the hypervalent chromium intermediates remained largely unknown. Here we report a detailed mechanistic picture for the formation and decomposition of Cr(IV) intermediates. Reactions of GSH with Cr(VI) are carried out in an excess of the oxidized form of glutathione (GSSG) in order to maintain constant pH during the reaction. Although we have chosen experimental conditions that are different from those in earlier studies, our conclusions may extend to those systems.

Experimental Section

Materials. Stock solutions of potassium dichromate were prepared in water from primary standard grade material. Glutathione (oxidized and reduced form) (Sigma) and 5,5-dimethylpyrroline *N*-oxide (DMPO) (Aldrich) were used without further purification. Sodium perchlorate was prepared by neutralization of Na_2CO_3 with $HClO_4$. Cation- (Dowex 50W-X4) and anion-exchange (Dowex 1X2-400) resins were pretreated before use.[22] Chromium(III) content was estimated by hydrogen peroxide oxidation in alkaline solution.[23] Sodium bis(2-hydroxy-2-ethylbutyrato)oxochromate(V) was prepared following the method of Krumpolc and Rocek.[16]

Stoichiometry Measurements. The reactions between Cr(VI) and excess glutathione (GSH) in the absence of added oxidized glutathione (GSSG) were carried out at pH 2.35. In a typical experiment, 1.0×10^{-2} g of GSH was added to a solution of 0.16 mL of 1.0×10^{-2} M $K_2Cr_2O_7$ and the total volume was adjusted to 10 mL. The reaction mixture was allowed to stand for 2 h at 25 °C. Following the completion of the reactions, unreacted glutathione (GSH) was estimated by iodate titration.[24]

Separation of Chromium(III) Products. The chromium(III) products obtained at the end of the Cr(VI)–glutathione reaction were charged onto anion- and cation-exchange columns separately. A column temperature of ~4 °C was maintained by circulating ice cold water in order to minimize decomposition of the Cr(III) products, which is generally observed for carboxylato Cr(III) complexes.[17-19,25] The green product(s) passes through the anion-exchange column quickly but is readily adsorbed onto the cation-exchange resin. A major portion of the product (>70%) was eluted by 1.0 M $HClO_4$, and the remainder suffered decomposition in the column, as evidenced by the familiar appearance of blue $Cr(H_2O)_6^{3+}$ complex. The eluant exhibits bands at 571 (ϵ = 28 M^{-1} cm^{-1}) and 408 nm (ϵ = 24 M^{-1} cm^{-1}). The product after separation also underwent slow decomposition ($t_{1/2}$ ~ 15 min), as evidenced by the change in absorbance and hypsochromatic shift of the 571-nm band with time.

Estimation of Glutathione (GSH) Attached to Chromium(III) Products. After the completion of the redox reaction, the pH of the chromium(VI) (6.5×10^{-5} mol) and glutathione (6.5×10^{-4} mol) reaction mixture (10 mL) was raised to 4.5 from its initial value, 2.7. The mixture was then charged onto an anion-exchange column in which excess unreacted glutathione was adsorbed and through which Cr(III) products passed quickly. The column was washed with water (2 × 5 mL). Washings and Cr(III) products were collected, and 2 M H_2SO_4 (10 mL) was added to this mixture. After 1 h, following the deligation of Cr(III) products, free GSH was estimated by iodate titration.[24]

Estimation of GSSG Attached to Chromium(III). The free oxidized form of glutathione was analyzed by a HPLC method utilizing a C_{18} reversed-phase column. HPLC separations were carried out either on a ternary gradient system (ISCO) interfaced with an IBM PS/2 microcomputer or on a Waters HPLC system (Model 994) equipped with a photodiode array detector. The disulfide absorbs significantly at 267 nm whereas the reduced form shows negligible absorption. In a typical analysis, 10 μL of the reaction mixture containing 0.01 M Cr(VI) and 0.1 M GSH was subjected to HPLC separations following the completion of the redox reaction. These isocratic separations were accomplished by either $H_3PO_4/H_2PO_4^-$ (50 mM, pH 3.0) or $HCOOH/HCOO^-$ buffers (50 mM, pH 3.0). The free oxidized form was well separated from other products (Figure 2). Concentrations were then calculated from peak areas utilizing calibrated values for standard samples. The coordinated GSSG was then estimated by subtracting from the total as expected from the iodate titrations.

Rate Measurements. Redox reactions between the thiol and dichromate were monitored spectrophotometrically on a computer-interfaced (Epson Equity 1+) UV–visible (Perkin–Elmer Lambda 600) spectrophotometer. The reaction was followed at 375, 460, 510, and 580 nm using at least 10-fold excess of tripeptide over Cr(VI). The absorbance vs time traces at 580 nm exhibit an exponential growth in absorbance, and the rate constant was evaluated from usual first-order plots ($\ln (A - A_\infty)$ vs time, where A and A_∞ are the absorbances at time t and at infinite time). Such first-order plots were linear for more than 4 half-lives. Kinetic traces at 460 and 510 nm exhibited an initial increase followed by a decrease in absorbance, whereas at 375 nm a decrease in absorbance was observed. This monotonic decrease, however, cannot be described by a single exponential decay. All these traces (375, 460, and 510 nm) can be adequately described by a pair of consecutive first-order reactions:

$$\mathrm{Cr(VI)} + \mathrm{GSH} \xrightarrow{k_0} \text{intermediate}$$

$$\text{intermediate} \xrightarrow{k'_0} \text{products}$$

The rate constants (k_0 and k'_0) and molar absorptivity of the intermediate (ϵ_I) were evaluated from a nonlinear least-squares iterative computer fit of the equation[26]

$$A = A_0 e^{-k_0 t} + \frac{[\mathrm{A}]_0 \epsilon_I k_0}{k'_0 - k_0}(e^{-k_0 t} - e^{-k'_0 t}) + \frac{A_\infty}{k'_0 - k_0}(k_0 e^{-k'_0 t} - k'_0 e^{-k_0 t}) + A_\infty \quad (1)$$

In this expression, A_0, A, and A_∞ are the absorbances at $t = 0$, at time t, and at infinite time; $[\mathrm{A}]_0$ represents initial [Cr(VI)]. It has been shown that any rate profiles dealing with the buildup and decay of an absorbing intermediate by first-order processes can be described by a pair of solutions having the same numerical values for the rate constants, but with the order of the assignment reversed.[27a] The molar absorptivity of the intermediate, however, will be different. All rate constants can be reproduced to better than 6%.

Magnetic Susceptibility Measurements of Intermediates and Products. The molar susceptibilities of the intermediates and products and the rates of their formation are determined utilizing a newly developed NMR method based on solution susceptibility measurements.[20] These experiments were carried out on a 300-MHz instrument (GE GN 300) equipped with variable-temperature probes. In a typical experiment, 1.0–2.0 mM Cr(VI) was mixed with excess glutathione (10–40 mM) in 10% D_2O solution containing appropriate buffer and $NaClO_4$. The frequency of the solvent H–O–D signal with time was monitored using

(16) Krumpolc, M.; Rocek, J. *J. Am. Chem. Soc.* **1979**, *101*, 3206–3209.
(17) Bose, R. N.; Gould, E. S. *Inorg. Chem.* **1985**, *24*, 2645–2647; **1985**, *24*, 2833–2835; **1986**, *25*, 94–97.
(18) (a) Fanchiang, Y.-T.; Bose, B. N.; Gelerinter, E.; Gould, E. S. *Inorg. Chem.* **1985**, *24*, 2833–2836. (b) Bose, R. N.; Rajasekar, N.; Thompson, D. M.; Gould, E. S. *Inorg. Chem.* **1986**, *25*, 3349–3353. (c) Ghosh, S. K.; Bose, R. N.; Laali, K.; Gould, E. S. *Inorg. Chem.* **1986**, *25*, 4737–4740. (d) Bose, R. N.; Neff, V. D.; Gould, E. S. *Inorg. Chem.* **1986**, *25*, 165–168.
(19) Ghosh, S. K.; Bose, R. N.; Gould, E. S. *Inorg. Chem.* **1987**, *26*, 899–903; **1987**, *26*, 3722–3727; **1987**, *26*, 2684–2687; **1987**, *26*, 2688–2692; **1988**, *27*, 1620–1625.
(20) Bose, R. N.; Li, D.; Moghaddas, S. *Anal. Chem.* **1991**, *63*, 2757–2762.
(21) An initial communication dealing with characterization of hypervalent chromium species utilizing this NMR method has already appeared: Bose, R. N.; Moghaddas, S.; Li, D. *Mendeleev Commun.* **1991**, 108–110.
(22) Gould, E. S. *J. Am. Chem. Soc.* **1967**, *89*, 5792–5796. The anion-exchange resin was pretreated as described, except that HCl was used instead of $HClO_4$.
(23) Haupt, G. W. J. *Res. Natl. Bur. Stand., Sect. A* **1952**, *48*, 414–423.
(24) Woodward, G. E.; Fry, E. G. *J. Biol. Chem.* **1932**, *97*, 465–471.
(25) Butler, R. D.; Taube, H. *J. Am. Chem. Soc.* **1965**, *87*, 5597–5602.
(26) Bose, R. N.; Viola, R. E.; Cornelius, R. D. *J. Am. Chem. Soc.* **1984**, *106*, 3336–3343.
(27) (a) See, for example: Alcock, N. W.; Denton, D. J.; Moore, P. *Trans. Faraday Soc.* **1970**, *60*, 2210. Frost, A. A.; Pearson, R. G. *Kinetics and Mechanism*, 3rd ed.; Wiley: New York, 1961; p 167. Espenson, J. H. *Chemical Kinetics and Reaction Mechanisms*; McGraw-Hill: New York, 1981; p 69–70. (b) Molar absorptivities of intermediates and products are equal at the delayed isosbestic point. Taking $\epsilon_I[A_0] = A_\infty$, it can be shown that eq 1 reduces to the conventional first-order equation:

$$A = (A_0 - A_\infty)e^{-k_0 t} + A_\infty$$

a data acquisition subroutine, "Kinet". In this acquisition procedure, free induction decays were collected at preprogrammed time intervals. At the end of the acquisitions, these FIDs are retrieved and transformed to spectra. The frequencies of the H–O–D signal with time were then tabulated. Since a single scan was sufficient to generate resonances with a signal to noise ratio greater than 100, pulse delays were not necessary. Usually, acquisition times were in milliseconds and were negligible in comparison to the reaction time.

The change in resonance frequency of a specific solvent resonance with time during a redox reaction is related to the rates of formation and disappearance of the paramagnetic centers and their molar susceptibilities. For example, if two diamagnetic reactants produce paramagnetic intermediates and products, the change in frequency with time exhibits a biphasic kinetic profile following the expression:

$$\Delta\nu = a_1 e^{-k_0 t} + a_2 e^{-k'_0 t} + a_3 \quad (2)$$

where k_0 and k'_0 are the rate constants for the formation of the intermediate and its decay. The parameters, a_1, a_2, and a_3 are related to

$$a_1 = \frac{4\pi\nu C}{3(k'_0 - k_0)}(\chi'_I k_0 - \chi'_P k')$$

$$a_2 = \frac{4\pi\nu k_0 C}{3(k'_0 - k_0)}(\chi'_P - \chi'_I)$$

$$a_3 = \frac{4\pi\nu C\chi'_P}{3}$$

in which C is the initial concentration of Cr(VI) (mol/mL) and χ'_I and χ'_P are the uncorrected molar susceptibilities of the intermediates and products. These uncorrected molar susceptibilities can be corrected by using

$$\chi^C = \chi' + \chi_S^M - \chi_{dia} \quad (3)$$

where χ^C is the corrected susceptibility, χ_S^M is the mass susceptibility of the solvent times the molecular mass of the paramagnetic substance, and χ_{dia} is the diamagnetic correction term. By using a nonlinear least-squares iterative computer fit of eq 2, we obtained the values of a_1, a_2, and rate constants. The uncorrected molar susceptibilities of the intermediates and products were then calculated utilizing the values of these constants. The reproducibility of rate constants is within 6% and the susceptibility can be reproduced to better than 5%. The rate constants obtained from the NMR measurements are in good agreement with the values obtained from the absorbance–time traces.

Electron Spin Resonance Measurements. Electron spin resonance measurements were carried out on an IBM 200D-SRC spectrometer operating in the X-band frequency (9.5 GHz) utilizing a flat quartz cell. The spectrometer frequency was measured using a Hewlett Packard 5351A microwave frequency counter, and the magnetic field was measured by the Hall probe of the spectrometer which has been previously calibrated near $g = 2$ using a NMR gaussmeter. The IBM ESR software was used to calculate g values, line widths, and line separations. Typical experimental parameters were as follows: data points, 4K; center of the frequency, 3400 G; sweep width, 200 G; acquisition time, 100 s; modulation frequency, 100 kHz; modulation amplitude, 5.01 G/pp; attenuation, 20 dB.

Experiments were initiated by mixing the tripeptide and chromium(VI) species at the desired pH and ionic strength and then placing it in the ESR tube. The spectra were then recorded immediately after mixing and at regular time intervals. The ESR spectra of the anionic Cr(V) complex, bis(2-ethyl-2-hydroxybutyrato)oxochromate(V), were also recorded at concentrations and pH values comparable to those used for the peptide reactions.

Results

Titration data based on the determination of unreacted GSH (Table I) reveal that 3.0 ± 0.1 mol of GSH are consumed for each mol of Cr(VI). HPLC separations indicate that the oxidized product has a retention time identical to that of GSSG. The reaction between Cr(VI) and GSH can then be written as

$$2HCrO_4^- + 6GSH + 8H^+ = 2Cr^{III} + 3GSSG + 8H_2O \quad (4)$$

Results of iodate titrations performed on Cr(III) products following the ion-exchange separations and subsequent treatment with H_2SO_4 are also tabulated in Table I. The spectral changes associated with the glutathione reduction of Cr(VI) in the presence of an excess of the oxidized form of glutathione (pH = 2.7) is shown in Figure 1. The spectra indicated the formation of an intermediate with a broad absorption band centered around 440 nm. The overlayed spectra exhibit a delayed isosbestic point at 580 nm. The products exhibit two bands in the visible spectra centered at 572 (ϵ = 33 M^{-1} cm^{-1}) and 408 nm (ϵ = 26 M^{-1} cm^{-1}). These spectroscopic features are also consistent with the formation of Cr(III) products.

Figure 2 shows HPLC profiles of the reaction mixture at various time intervals. The longest retained species (peak IV) in the column is the free oxidized glutathione. Independent determinations of the retention times of the Cr(VI) reactant and of the Cr(III) products reveal that these two oxidation states have close retention times (150 s for Cr(III) and 155 s for Cr(VI)). Peak I represents the mixture of the two oxidation states during the reaction and Cr(III) alone at the end of the reaction. Two other peaks, II and III, which grow and then decay with time represent the intermediates. These intermediates were also detected at 460 nm as the only peaks since Cr(VI), Cr(III), and GSSG do not absorb significantly at this wavelength. The inset in Figure 2 displays the chromatogram recorded at 460 nm. The remaining minor peak, V is due to an impurity in the GSH sample. The spectra for both II and III, recorded rapidly (20-ms acquisition time) during HPLC separations utilizing a diode array detector, exhibit a band centered around 460 nm. Quantitative estimations of free GSSG from the chromatograms based on the standard

Table I. Estimations of GSH Consumed, GS^-, and GSSG Attached to Cr(III) in the Reaction[a] between Cr(VI) and GSH at 25 °C

10^6[Cr(VI)] employed, mol	10^6[GSH] employed, mol	10^6[GSH] oxidized, mol	10^6[GSH] attached to Cr(III), mol	10^6[GSSG] free, mol
		A. Iodate Titration[b]		
3.26	32.6	9.8		
3.26	32.6	9.7		
3.26	32.6	9.9		
		B. Iodate Titration Following Ion-Exchange Separations and Deligation[c]		
65.0	650		82	
65.0	650		85	
65.0	650		80	
		C. HPLC Analysis[d]		
5.0×10^{-2}	5.0×10^{-1}			5.2×10^{-2}
5.0×10^{-2}	5.0×10^{-1}			4.8×10^{-2}
5.0×10^{-2}	5.0×10^{-1}			5.1×10^{-2}

[a] In the absence of added GSSG. [b] At pH 2.35. [c] At pH 2.70. [d] At pH 2.70.

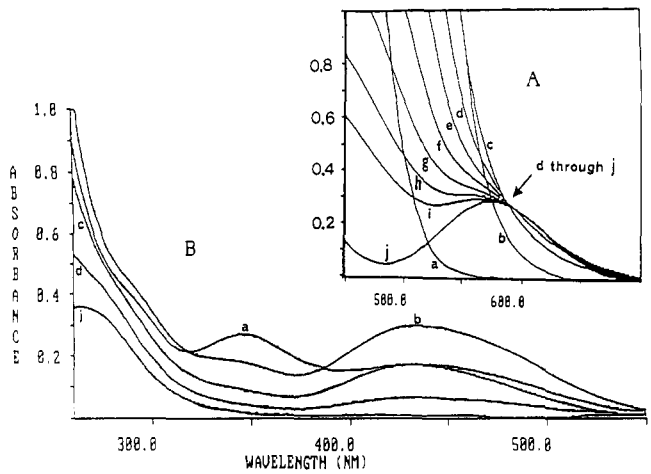

Figure 1. (A) Overlapped absorption spectra of the glutathione (50 mM)–Cr(VI) (10 mM) reaction mixture at pH = 2.60 (μ = 0.5 M adjusted with $NaClO_4$) at various time intervals: (a) Cr(VI) alone; (b) reaction immediately after mixing; (c–i) reaction recorded at 1-min intervals; (j) reaction upon completion (~2 h). Note that (b) through (e) are off scale below 450 nm, and spectra exhibit a delayed isosbestic point at 580 nm. (B) Overlayed spectra in the wavelength range 550–250 nm using [Cr(VI)] = 2.0×10^{-4} M; [GSH] = 0.01 M. Other conditions and labeling correspond to those in (A).

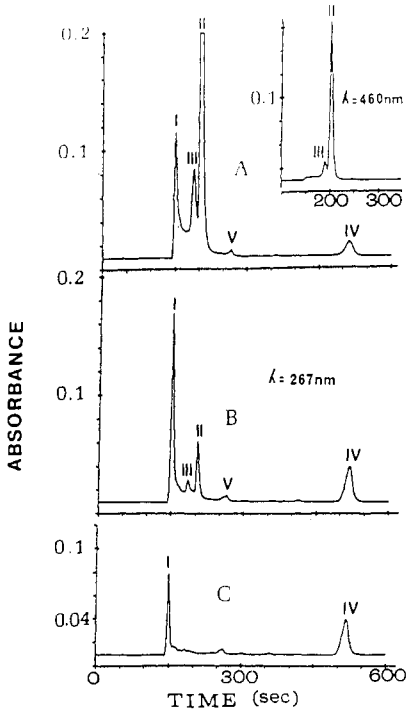

Figure 2. High-performance liquid chromatograms for Cr(VI) (0.01 M) plus GSH (0.1 M) recorded at various time intervals using a C_{18} reversed-phase column. Conditions: mobile phase, $H_3PO_4/H_2PO_4^-$ buffer (50 mM); flow rate, 1 mL/min; sample size, 10 μL. Chromatograms A, B, and C were recorded at 267 nm immediately following the injections of the samples, after 3 min, and after 13 min of mixing. The inset is the detector response at 460 nm for chromatogram A. Peak assignments are as follows: (I) Cr(VI) + Cr(III) products; (II) Cr(IV) species; (III) Cr(V) species; (IV) free GSSG; (V) an impurity. Peak II is set off scale in (A) in order to show other smaller peaks in the chromatogram.

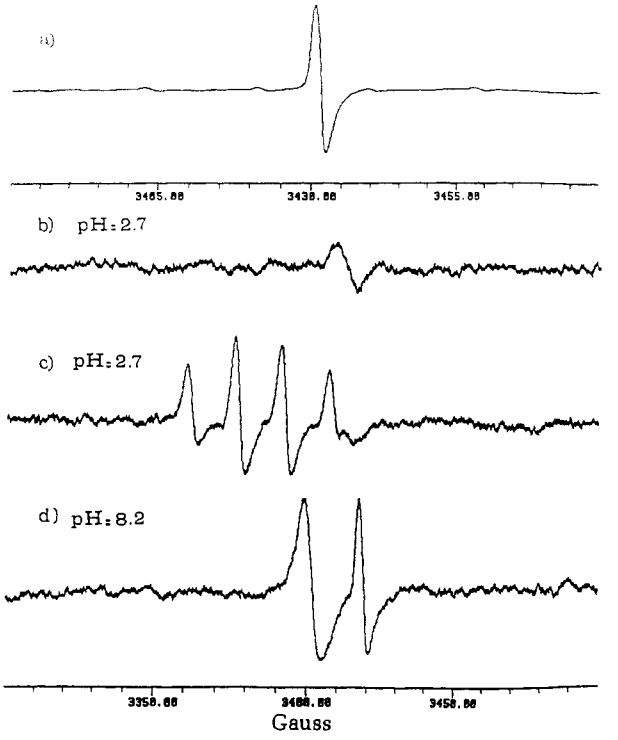

Figure 3. ESR spectra of various Cr(V) species and the DMPO–thiyl radical: (a) bis(2-hydroxy-2-ethylbutyrato)oxochromate(V) anion (1.0 mM) at pH 3.0; (b) a chromium(V) intermediate during the Cr(VI) (5.0 mM)–glutathione (50 mM) reaction in GSSG (50 mM) and $NaClO_4$ (0.5 M) solution at pH 2.7; (c) DMPO–thiyl radical for the same reaction as in (b) except that [DMPO] = 53 mM; (d) two Cr(V) intermediates at pH 8.2 (other conditions are the same as in (b)).

Table II. ESR Parameters for Various Cr(V) Species and the DMPO–Thiyl Radical

species	pH	*g* values	hyperfine coupling constant, G
$[Cr(EBA)_2(O)]^-$ [a]	3.0	1.978	18
Cr(V) Int(1)[c,d]	2.7	1.989	
	7.1	1.985	
	8.2	1.985	
Cr(V) Int(2)[c,d]	2.7		
	7.1	1.995	
	8.2	1.995	
DMPO–thiyl radical	2.7	2.005	15.5[e]
	7.1	2.006	15.6[e]

[a] EBA = 2-hydroxy-2-ethylbutyrate dianion. [b] Coupling with ^{53}Cr ($I = {}^3/_2$, 9.54% natural abundance). [c] Int(1) and Int(2) refer to two Cr(V) intermediates, and no coupling with ^{53}Cr was observed due to weak signal intensities. [d] [Cr(VI)] = 5.0 mM, [GSH] = 50 mM, [$NaClO_4$] = 0.5 M. [e] Coupling with pyrroline nitrogen and protons.

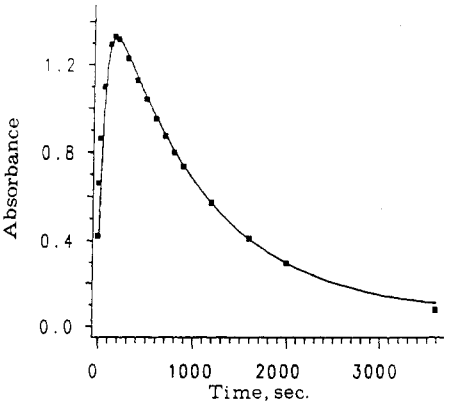

Figure 4. Typical absorbance time trace (at 460 nm) for the glutathione (10 mM)–Cr(VI) (1 mM) reaction in excess GSSG (0.05 M), pH 2.64, μ = 0.5 M. The experimental curve is represented by a solid line, and the calculated absorbances (according to eq 1) are shown by solid squares. The computer-simulated data correspond to $k_0 = 0.016\ s^{-1}$, $k'_0 = 9.5 \times 10^{-4}\ s^{-1}$, $\epsilon_I = 1550\ M^{-1}\ cm^{-1}$, and $A_\infty = 0.057$.

calibration curves of pure GSSG samples are reported in Table I.

The reaction mixtures containing Cr(VI) (2–10 mM) and glutathione (20–50 mM) in the presence and absence of GSSG initially (2–5 min after mixing) at pH 2.7 exhibited a weak ESR signal at $g = 1.989$, which slowly (in 10–30 min) disappeared. At higher pH however, Cr(VI)–glutathione reaction mixtures exhibited two intense signals at $g = 1.985$ and 1.995, which grew initially and then decayed. In the presence of DMPO, strong four-line signals with an average coupling constant of 15.6 G (Figure 3) were observed at the onset of the reaction in all pH values (2–8). An authentic anionic Cr(V) complex, bis(2-hydroxy-2-ethylbutyrato)oxochromate(V), $[Cr(O)(EBA)_2]^-$, on the other hand, exhibited an intense signal at $g = 1.998$, even at 0.5 mM concentration in acidic (pH = 2 to 3.5) aqueous solutions. The ESR spectrum of this complex exhibits hyperfine couplings with ^{53}Cr nuclei (9.54% abundance; $I = {}^3/_2$). Table II reports the *g* values and coupling constants for intermediates and the $[Cr^V(O)(EBA)_2]^-$ complex.

The reaction of Cr(VI) with GSH exhibited a biphasic kinetic profile at all wavelengths except at the delayed isosbestic point at 580 nm. At the latter wavelength an exponential growth in absorbance was observed from which the first-order rate constant was evaluated. Figure 4 shows observed and computer-simulated absorbance–time profiles for the redox reaction at 460 nm. Two rate constants which were evaluated by treating kinetic profiles as two consecutive first-order reactions are listed in Table III. As indicated in the Experimental Section, there are two solutions for these biphasic profiles. For example, one solution afforded the molar absorptivity of the intermediate, 1550 $M^{-1}\ cm^{-1}$, along with the rate constants for the formation of the intermediate and its decay as 0.016 and $9.5 \times 10^{-4}\ s^{-1}$. An identical curve can be

Table III. Rate Data for the Redox Reaction of Cr(VI)[a] with Glutathione in the Presence of Excess Oxidized Form of Glutathione[b] at 25.0 °C and μ = 0.5 M ($NaClO_4$)

[GSH], mM	pH	$10^{-3}\epsilon_I$,[d,f] M^{-1} cm^{-1}	10^3k_0,[c] s^{-1}	$10^4k'_0$,[e] s^{-1}
0.5	2.64		1.5 (1.3)	0.37 (0.7)
1.0	2.66	1.0	2.2 (2.4)	0.89 (1.4)
2.7	2.68	1.2	5.1 (5.0)	4.2 (3.8)
5.0	2.68	1.5	7.3 (7.8)	6.0 (7.1)
10.0	2.76	1.6	14 (13)	11 (14)
15.0	2.72	1.7	18 (18)	16 (21)
20.0	2.71	1.7	22 (22)	29 (28)
30.0	2.70	1.6	30 (31)	48 (43)
40.0	2.69	1.6	42 (40)	53 (57)
50.0	2.70	1.6	50 (49)	76 (71)
60.0	2.68	1.8	57 (58)	83 (85)
10.0	1.71	1.7	70	14
10.0	2.18	1.6	39	11
10.0	2.70	1.6	16	9.5
10.0	2.76	1.6	14	11
10.0	3.32	1.7	6.5	13
25.0	2.70	1.5	31	60[g]
25.0	2.70		28	54[g,h]

[a] [Cr(VI)] = 5×10^{-5} to 1.0×10^{-3} M. [b] Total GSSG concentration was kept invariant at 0.05 M; distribution to the protonated (carboxylic acid) and deprotonated forms depends on pH. [c] Values in parentheses are calculated from the rate law (5a) using $k_{et} = 7.3 \times 10^{-3}$ s^{-1}, $k_2 = 0.89$ M^{-1} s^{-1}, and $K = 4.0 \times 10^{-2}$ M^{-1}. [d] At 460 nm. [e] Calculated values are in parentheses according to $k'_0 = k$[GSH] using $k = 0.13$ M^{-1} s^{-1}. [f] Maximum Cr(IV) concentrations vary between 65 and 80% of the initial Cr(VI) concentration. [g] In the absence of GSSG. [h] Evaluated using the NMR method.

simulated with $\epsilon_I = 2.06 \times 10^4$ M^{-1} cm^{-1} when the assignment of the rate constant is reversed, i.e., 9.5×10^{-4} and 0.016 s^{-1} are taken as the rate constants for the formation and decomposition of the intermediate. The rate constant evaluated at the delayed isosbestic wavelength at 580 nm agrees with the larger rate constant in the biphasic solution.[27b] We therefore assign k_0 to the formation of the intermediate and k'_0 to its decay.

First-order rate constants for the formation of the intermediates[28] in the presence of added GSSG increase with the increasing [H^+] and exhibit complex dependence on [GSH] (Figure 5). While there is a linear dependence of k_0 on [GSH] above 0.01 M, there is a non-zero intercept, and points at lower [GSH] demonstrate a sharp curvature in the plot. The rate data can be described by eq 5. A nonlinear least-squares treatment of the

$$k_0 = \frac{(a + b[\text{GSH}])[\text{GSH}]}{1 + c[\text{GSH}]} \qquad (5)$$

rate data yielded $a = 3.0 \pm 0.2$ M^{-1} s^{-1}, $b = (3.6 \pm 0.3) \times 10^2$ M^{-2} s^{-1}, and $c = (4.0 \pm 0.3) \times 10^2$ M^{-1}. The smooth line in Figure 5 is calculated using these values. The experimental rate constants, along with the values calculated according to eq 5, are given in Table III.

Intermediates are reduced to Cr(III) products. Although appreciable random scattering in the k'_0 vs [GSH] plot was apparent, especially in the low thiol concentrations, a second-order reaction, first-order with respect to both intermediate and tripeptide, is perhaps the best description for the decomposition of the intermediate. The second-order rate constant was calculated to be 0.13 M^{-1} s^{-1} at pH 2.70, utilizing a linear least-squares fit of the equation $k'_0 = k$[GSH]. The calculated values are listed in parentheses in Table III next to the experimental rate data. These second-order rate constants exhibit no significant pH dependence in the range 1.8–3.3. At other pH values the same constant was calculated by dividing k'_0 with [GSH].

The rate constants were also evaluated from the solvent resonance frequency vs time curves by using eq 2. Usually, a net change in frequency of 17–18 Hz was observed during the redox reaction by utilizing 2.0 mM Cr(VI). A typical frequency–time curve is shown in Figure 6. The rate constants obtained from the computer fits of eq 2 are compared with those evaluated from the conventional absorbance–time traces in Table IV. As can be seen, the rate data obtained from the two methods agree. For example, utilizing 1.0 mM Cr(VI) and 10.0 mM glutathione in 50 mM GSSG, two rate constants, 0.015 and 1.2×10^{-3} s^{-1}, were obtained from the frequency–time data, in excellent agreement

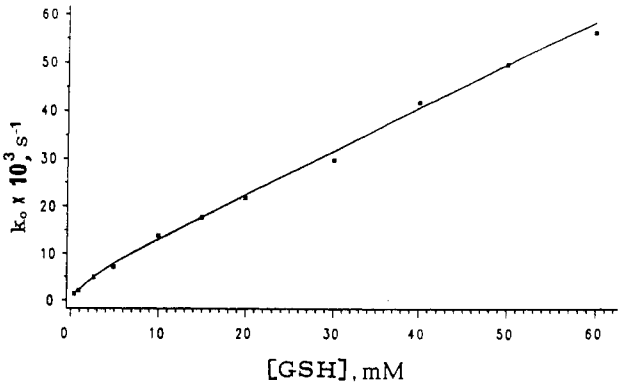

Figure 5. Variation of first-order rate constant (k_0) as a function of [GSH] at pH = 2.7, μ = 0.5 M, in the presence of GSSG (0.05 M). The solid line is the computer-simulated line according to eq 5, and solid squares are measured rate constants. The computer-simulated curve corresponds to $a = 3.0$ M^{-1} s^{-1}, $b = 3.6 \times 10^2$ M^{-2} s^{-1}, and $c = 4.0 \times 10^2$ M^{-1}.

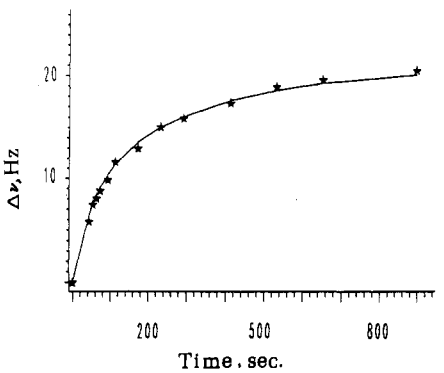

Figure 6. Observed (asterisk) and simulated (solid line) $\Delta\nu$–time curves for the Cr(VI) (2.0 mM)–GSH (20.0 mM) reaction in the presence of GSSG (50.0 mM) at pH 2.70, μ = 0.5 M ($NaClO_4$), T = 25 °C. The simulated curve is according to eq 2 utilizing $a_1 = -8.29$, $a_2 = -11.66$, $a_3 = 19.95$, $k_0 = 1.9 \times 10^{-2}$ s^{-1}, and $k'_0 = 3.2 \times 10^{-3}$ s^{-1}.

Table IV. Comparison of Rate Constants[a] Evaluated from Biphasic Profiles Utilizing UV–vis and NMR Methods in the Presence of GSSG (50 mM), pH = 2.7, μ = 0.5 M, T = 25 °C

[GSH], mM	UV–vis method		NMR method	
	10^3k_0, s^{-1}	$10^4k'_0$, s^{-1}	10^3k_0, s^{-1}	$10^4k'_0$, s^{-1}
10.0	14	11	15	12
20.0	22	29	19	32
40.0	42	53	42	54
25.0[b]	31	60	28	54

[a] [Cr(VI)] lies in the range 1–2.5 mM. [b] In the absence of added GSSG.

(28) (a) The term intermediate is exclusively used to designate species which are formed and decayed on longer time scales and for which the rates of formation and decomposition are measured. Although an initial intermediate, a Cr(VI)–glutathione complex formed immediately after mixing the reactants is described as a Cr(VI)–thioester complex. (b) All rate measurements (except for one measurement) were carried out in an excess of GSSG. A change in pH up to 0.3 unit was observed when Cr(VI):GSH was 1:10 in the absence of extra GSSG. This primarily reflects the need, in the redox reaction, of four H^+ per Cr(VI). These protons must be transferred from GSH or GSSG (mostly from carboxylic acid groups) to the chromium center, and therefore the conjugate acid:base ratio of the peptide is expected to change significantly in the absence of additional GSSG with low Cr(VI):GSH. When extra GSSG is added, the change in the ratio (acid:base) during the redox reaction is minimal and hence no significant change in pH is observed.

with the values 0.014 and 1.1×10^{-3} s^{-1} resolved from the absorbance–time data under identical conditions. By using the values of a_3 and the preexponential factors, a_1 and a_2 in eq 2, the uncorrected molar susceptibilities of the intermediates and products were calculated. Under the conditions stated above, molar susceptibilities of the intermediates and products are estimated as 3.4×10^{-3} and 6.9×10^{-3} cm^3/mol. Although molecular masses and compositions are required to calculate the corrected susceptibility, the correction factors (eq 3) usually account for no more than 5% of the uncorrected values. For example, under the assumption that in the product two GS^- and two H_2O molecules are attached to Cr, χ_S^M and χ_{dia} are calculated to be -5.0×10^{-4} and -3.3×10^{-4} cm^3/mol. A net correction of -1.7×10^{-4} cm^3/mol (eq 3), which is 2.5% of the uncorrected value, should be made. In light of this limitation, the spin-only magnetic moments for these species were calculated to be in the range 2.8–3.0 μ_B for intermediates and 3.8–4.1 μ_B for products utilizing uncorrected susceptibility values.

Discussion

Nature of the Intermediates and Product. At lower pH, only a weak ESR signal for the intermediate was observed, starting with 2–10 mM Cr(VI), even at times when the concentration of the intermediate is expected to be maximum (80% of the initial Cr(VI) concentration). On the other hand, the Cr(V) complex, $[Cr(O)(EBA)_2]^-$, exhibits an intense signal at this pH with submillimolar concentrations. Chromium(IV) species usually do not exhibit an ESR signal at room temperature (reflecting large zero-field splitting and spin–orbit couplings). Taking the calibrated intensity data of the known Cr(V) complex (with the assumption that these Cr(V) complexes are equally ESR sensitive), we estimate that less than 3% of the intermediate is Cr(V). The magnetic moments of the intermediates lie in the range 2.8–3.0 μ_B, i.e. close to the value expected for two unpaired electrons. The magnetic moment along with the ESR data unambiguously establish that Cr(IV) is the dominant detectable intermediate. A small amount of Cr(V) (<5%) also exists as a minor intermediate at pH 2.7. HPLC separations also reveal that two intermediates grow initially and then decay to products. The intensity ratio of these two signals reaffirms the existence of a major Cr(IV) and a minor Cr(V) (peaks II and III in Figure 2) intermediate with the assumption that the molar absorptivities of these two species are not drastically different from each other.

The weak ESR signal at $g = 1.997$ matches with the Cr(V) signal observed by Goodgame and Joy[10] for the Cr(VI)–glutathione reaction at higher [GSH] ([GSH]/[Cr(VI) > 2). These authors attributed this signal to a bis(glutathionato)Chromium(V) complex. The formation of a thiyl radical is also apparent from the detection of four-line ESR signals utilizing DMPO, a spin trap for radicals.[2] The DMPO–SG radical adduct is shown to exhibit couplings[2] with both nitrogen (coupling constant = 15.0 G) and hydrogen atoms (coupling constant = 16.3 G). The line width of the DMPO radical adduct that we have observed is more than 2 G, and therefore individual couplings were not observed. However, an intensity distribution of 1:2:2:1 along with an average coupling constant of 15.6 G would be in keeping with the splitting diagram in which both the nitrogen and hydrogen atoms were involved in couplings with nearly the same coupling constant.

The electronic absorption spectra of the Cr(III) products in the presence of GSSG or in excess GSH (self-buffered) do not exhibit marked differences in absorption maxima or in extinction coefficients, as shown in Table V. The absorption maxima and molar absorptivities of the eluants are comparable to the products in solution prior to separation except that further decomposition of Cr(III) products takes place during separation. This slow decomposition ($t_{1/2} \sim 15$ min) prohibits our formulating the exact composition of the complex. However, we note that products are monocationic complexes, as evidenced by the ion-exchange behavior. HPLC and titration data show that at least one GSH and half of a GSSG molecule are attached to a Cr(III) center. The coordination of the GSSG molecule must have taken place during the reduction process, since substitution onto the Cr(III) center is sluggish and the chromium(III) product contains the oxidized molecule when the reaction was carried out in its absence. A dinuclear Cr(III) product containing one GSSG and two GSH molecules per dimer is consistent with the HPLC, cation-exchange, and titration data and with the mechanism proposed here.

Table V. Visible Spectral Features for the Cr(III) Products of the Cr(VI)–Glutathione Reaction

buffer	λ^1_{max} (ϵ), nm (M^{-1} cm^{-1})	λ^2_{max} (ϵ), nm (M^{-1} cm^{-1})
GSSG	572 (33)	408 (26)
	571 (28)[a]	413 (24)[a]
GSH	572 (33)	410 (26)

[a] Spectra were recorded immediately after separation (~5 min) from the cation-exchange column. Slightly smaller values in ϵ are a result of further decomposition of the products after separation. The extrapolated values at zero time are in good agreement with the corresponding values before separation.

Mechanism of Formation of Cr(IV) and Cr(V) Intermediates. Any proposed mechanism must account for the parallel formations of a minor Cr(V) and a major Cr(IV) species as detectable intermediates. Further, the mechanism must accommodate sequential one-electron transfer processes, since we observe healthy ESR signals for a thiyl radical adduct, the one-electron-oxidized product of the tripeptide. The rate law, ESR, and magnetic susceptibility data are consistent with the following mechanism:

$$GSH + Cr^{VI} \underset{k_{-1}}{\overset{k_1}{\rightleftharpoons}} Cr^{VI}(GS^-) + H^+ \quad (6)$$

$$Cr^{VI}(GS^-) \xrightarrow{k_{et}} Cr^V + GS^\bullet \quad (7)$$

$$Cr^{VI}(GS^-) + GSH \xrightarrow{k_2} Cr^V(GS^-) + GS^\bullet + H^+ \quad (8)$$

$$2GS^\bullet \xrightarrow{fast} GS\text{–}SG \quad (9)$$

$$Cr^V + GSH \xrightarrow{fast} Cr^V(GS^-) + H^+ \quad (10)$$

$$Cr^V(GS^-) + GSH \xrightarrow{fast} Cr^V(GS^-)_2 + H^+ \quad (10a)$$

$$Cr^V(GS^-) + GSH \xrightarrow{fast} Cr^{IV}(GS^-) + H^+ + GS^\bullet \quad (11)$$

Protons released from GSH are readily transferred to oxo (or hydroxo) groups attached to the metal center to form water. In addition, a rapid equilibrium between the mono(glutathionato)-chromium(IV) and bis(glutathionato)chromium(IV) complexes may exist. This step, as well as reactions 9–11, does not alter the rate law since none is a rate-limiting process. Following this mechanism, the observed first-order rate constants can be related to

$$k_0 = \frac{Kk_{et}[GSH] + Kk_2[GSH]^2}{1 + K[GSH]} \quad (5a)$$

where $K = k_1/k_{-1}$. By using the values of a, b, and c obtained from the nonlinear least-squares fit of the data in Figure 5 with eq 5, calculated values for K, k_{et}, and k_2 are 4.0×10^2 M^{-1}, 7.3×10^{-3} s^{-1}, and 0.89 M^{-1} s^{-1}.

An alternative to eq 5a can be derived by making a steady-state approximation on the $Cr^{VI}(GS^-)$ complex, giving eq 5b. By using

$$k_0 = \frac{\left(\frac{k_{et}k_1}{k_{-1} + k_{et}} + \frac{k_2k_1}{k_{-1} + k_{et}}[GSH]\right)[GSH]}{1 + \frac{k_2}{k_{-1} + k_{et}}[GSH]} = \frac{(k_{et}k_1 + k_2k_1[GSH])[GSH]}{k_{-1} + k_{et} + k_2[GSH]} \quad (5b)$$

the values of a, b, and c stated above, the calculated values of k_1 ($=b/c$) and k_2/k_{et} ($=b/a$) are 0.89 M^{-1} s^{-1} and 120 M^{-1}, respectively. If the expression for c is solved for k_{-1}/k_{et} and the calculated value for k_2/k_{et} is entered, one obtains $k_1/k_{et} = -0.27$, an impossible negative value. Thus, the Cr(VI)–thioester complex

maintains a rapid equilibrium with its reactants with concentrations much higher than expected from a steady-state approximation.

The rate of formation of the intermediates is reported in this mathematical form by McAuley and Olatunji[12] for the disappearance of Cr(VI). However, there are some mechanistic differences. First, we concur with these authors that a thioester complex is formed rapidly. In addition, we observe that Cr(IV) and Cr(V) species are major and minor long-lived intermediates in this reaction. These intermediates are formed by parallel reactions of the rapidly equilibrated thioester complex through an internal electron transfer and a direct one-electron reduction by a second molecule of GSH to yield Cr(V) complexes. The latter then react rapidly with the tripeptide, conceivably through two competing pathways: an electron-transfer reaction to form long-lived Cr(IV) and a substitution reaction to form (glutathionato)chromium(V) intermediates. Since both steps are rapid, they do not enter into the rate law. However, the rate ratio of these two steps determines the ratio of Cr(IV):Cr(V). The small ESR signal at $g = 1.997$ matches with the signal for the bis(glutathionato)chromium(V) species observed by Goodgame and Joy[10] at high glutathione concentration. We suspect that this bis(thiolato)chromium(V) complex has much higher longevity as compared to the mono(thiolato) and unligated Cr(V) complexes toward further reduction by the thiol ligand. At higher pH, both the bis- and mono(glutathionato) complexes are stabilized, and therefore two Cr(V) ESR signals can be detected. We also suggest that the Cr(IV) complexes are ligated by the tripeptide, since the substitution reaction is fast around this metal center. Although the Cr(IV) species is the dominant long-lived intermediate, sequential one-electron transfer takes place during the reaction, as evidenced by the detection of a DMPO–glutathione thiyl radical adduct. These results also support our mechanism in which the transient Cr(V) species reacts rapidly at lower pH with the tripeptide and therefore most of it escapes the detection by ESR spectroscopy.

Our kinetic analysis is in agreement with the mechanistic picture presented by Connett and Wetterhahn[13] who supported Cr(IV) species as the major intermediates in this reaction although these authors did not observe the additional internal electron-transfer pathway at higher pH. O'Brien and Ozolins[14] proposed a mechanism at neutral pH featuring an initial two-electron-transfer processes by two molecules of glutathione to form Cr(IV) species. This hypervalent species then underwent a rapid disproportionation reaction to form Cr(V) and Cr(III). Our data do not support such a mechanism in acidic solution. First, GSH is operating as a one-electron reductant since we have detected the one-electron oxidized product, i.e., the thiyl radical in the initial stage of the reaction. Chromium(V) must be a precursor of Cr(IV) if the redox reaction occurs in this stepwise manner. In any event, in the absence of appreciable ESR signals for Cr(V), we conclude that such a disproportionation reaction is much slower than further reduction by glutathione to form Cr(III) products in acidic solution. Since this reaction was carried out in excess glutathione, one needs to compare the rate of reduction of Cr(IV) by GSH with that for the disproportionation reaction. We have generated Cr(IV) intermediates[17-19] chemically and electrochemically using Rocek's Cr(V) complex[16] and investigated the redox reactions of this oxidation state with many metal and non-metal reductants including cysteine and thiolactic acids. Rate data for none of these redox reactions require that Cr(IV) is depleted by a disproportionation reaction in acidic solutions when excess reducing agent is present. The above arguments, however, do not rule out the possibility that at neutral and higher pH an initially generated Cr(V) species is rapidly reduced to Cr(IV) followed by a rapid base-catalyzed disproportionation of the latter to form a more stable Cr(V) (different from initial Cr(V)) and Cr(III) species. Although mechanisms of disproportionation of Cr(IV) complexes are largely unknown, disproportionation of Cr(V) complexes is indeed a base-catalyzed process.[29] In the absence of specific rate data for the disproportionation of Cr(IV) it would be speculative to choose a pathway for the formation of Cr(V) in neutral solution between two alternatives: (1) the direct reduction of Cr(VI) by GSH or (2) the disproportionation of Cr(IV).

The apparent formation constant for the Cr(VI)–thioester complex, reaction 6, was evaluated as 4.0×10^2 M^{-1} at pH 2.7. An analogous constant was determined[12,13] to be 1.4×10^3 and 21 M^{-1} at pH values <1 and 7.4, respectively. A similar increase in the rate of formation of the Cr(VI)–thioester complex with increasing $[H^+]$ has been reported by Connett and Wetterhahn[30] for a number of thiols. Therefore, the higher quotient (as well as rate constant) at high $[H^+]$ may reflect the efficient proton transfer to the chromate oxygen as documented by several workers[30-34] dealing with acid-catalyzed substitution reactions of Cr(VI). This observation also suggests that dissociation rates of the precursor complex do not increase as sharply with $[H^+]$ as does its formation rate.

The apparent molar absorptivity of the intermediate initially increases with the increase in [GSH] and then levels off at higher thiol concentrations. These data suggest that Cr(IV) is partitioned in two forms with the ratio of the forms governed by the ligand concentration. Alternatively, a change in the Cr(V):Cr(IV) ratio as a function of ligand concentration can be ruled out since the relative intensity of the ESR signals was independent of ligand concentration, as long as a 10-fold excess of ligand over Cr(VI) was maintained. Although an equilibrium constant of $(5 \pm 1) \times 10^2$ M^{-1} can be evaluated using these molar absorptivity data, such a value is highly imprecise since these values can be reproduced only to within 10%. The magnetic susceptibility data are not inconsistent with the existence of the two forms of Cr(IV) since they differ by only a small (<1% of the uncorrected molar susceptibility) diamagnetic correction term containing an additional glutathione molecule.

Mechanism of Decomposition of Chromium(IV). The long-lived intermediate is predominantly the Cr(IV) species. Therefore, the second phase of the reaction contains rate information regarding the decomposition of these species. A second-order rate constant of 0.13 M^{-1} s^{-1} was evaluated for the decomposition of these intermediates from least-squares treatment. From our analytical data we conclude that at least one GSH and half of a GSSG molecule are attached to a Cr(III) center. Since the coordinated GSSG was estimated in the absence of the added GSSG, the ligated GSSG must have come from the products. Further, coordinations by these peptides must have taken place prior to reduction, i.e., at the Cr(IV) level, since Cr(III) is substitution inert. The Cr(IV) intermediate proposed in eq 11 may be reduced to Cr(III) by a second GSH molecule through an inner-sphere mechanism with both GSH and GS$^\bullet$ attached to Cr(III). Two such Cr(III) units containing the thiyl radical may combine rapidly to form a dinuclear Cr(III) product which would be consistent with our analytical data. An internal electron transfer within a bis(glutathionato)chromium(IV) complex can be ruled out, for such a mechanism implies that the formation of the bis complex is the rate-limiting process and the second-order rate constant, 0.13 M^{-1} s^{-1}, is too small to account for a substitution reaction around the Cr(IV) center. A mechanism consistent with our data is

$$Cr^{IV}(GS^-) + GSH \xrightarrow{k} (GS^-)Cr^{III}\text{–}GS^\bullet + H^+ \qquad (12)$$

$$2(GS^-)Cr^{III}\text{–}GS^\bullet \xrightarrow{\text{fast}} (GS^-)Cr^{III}\text{–}GSSG\text{–}Cr^{III}(GS^-) \qquad (13)$$

The rate constants for Cr(IV) decomposition in the presence of GSSG are slightly smaller than those in its absence under identical

(29) Krumpolc, M.; Rocek, J. *Inorg. Chem.* **1986**, *24*, 617–621.

(30) Connett, P. H.; Wetterhahn, K. E. *J. Am. Chem. Soc.* **1986**, *108*, 1842–1847.

(31) Muirhead, K. A.; Haight, G. P., Jr.; Beattie, J. K. *J. Am. Chem. Soc.* **1972**, *94*, 3006–3010. Frennesson, S. A.; Beattle, J. K.; Haight, G. P., Jr. *J. Am. Chem. Soc.* **1968**, *90*, 6018–6022.

(32) Lin, C.; Beattie, J. K. *J. Am. Chem. Soc.* **1972**, *94*, 3011–3014.

(33) Swinehart, J. H.; Castellan, G. W. *Inorg. Chem.* **1964**, *3*, 278–280.

(34) Haim, A. *Inorg. Chem.* **1972**, *11*, 3147–3149.

conditions. Without additional data this small difference in the rate of decomposition does not allow us to conclude that the oxidized form further stabilizes the Cr(IV) species.

O'Brien and Ozolins[14] noted that at higher pH the dominant Cr(V) complexes decayed to Cr(III) products through a two-term rate law, a first-order process (first order in Cr(V); rate constant = 1.5×10^{-3} s^{-1}) and a second-order process (first order in each Cr(V) and GSH; rate constant = 9.1×10^{-3} M^{-1} s^{-1}). At higher pH it is likely that the Cr(V) species undergoes parallel internal electron transfer and a direct reaction by a GSH molecule to form the Cr(IV) complex. This Cr(IV) complex is then rapidly reduced to Cr(III) products, in accord with our rate data showing that the second-order rate constant for the chromium(IV) decomposition ($k = 0.13$ M^{-1} s^{-1}) in our system is at least 10 times larger than that for ($k = 9.1 \times 10^{-3}$ M^{-1} s^{-1}) the decomposition of Cr(V) complexes.[14]

Acknowledgment. Funding of this research by the Kent State University Research Council is gratefully acknowledged. We thank Professors Wetterhahn and Gould for valuable discussions and Mr. Sutisak Kitareewan for helping with the recording of "time of fly" spectra during the HPLC separations. We are also grateful to reviewer no. 3 for incisive comments and helping with stylistic changes of the manuscript.

Contribution from the Department of Chemical Pathology, Institute of Child Health, Red Cross War Memorial Children's Hospital, Rondebosch 7700, Cape Town, South Africa, and Department of Chemical Pathology, University of Cape Town Medical School, Observatory 7925, Cape Town, South Africa

Mechanism of Iron Release from Human Serum C-Terminal Monoferric Transferrin to Pyrophosphate: Kinetic Discrimination between Alternative Mechanisms

Timothy J. Egan,*,† David C. Ross,† Langley R. Purves,† and Paul A. Adams‡

Received February 11, 1992

The kinetics of iron release from C-terminal monoferric transferrin (Fe_CTf) to pyrophosphate (PP) under pseudo-first-order conditions show an apparent saturation linear dependence of k_{obs} on [PP]. The variation of k_{obs} with [PP] was studied under conditions of variable temperature and added anion (X) concentration (Cl^-, ClO_4^-, NO_3^-, SO_4^{2-}, HPO_4^{2-}). The results conform globally to a two-path mechanism (mechanism 1) involving iron removal either from a species with added anion bound to a kinetically significant anion binding (KISAB) site on the protein or with PP bound to the KISAB site, these two species being linked by a rapid equilibrium. Microscopic rate and equilibrium constants were evaluated by nonlinear regression of kinetic data to the equation $k_{obs} = (k_1[PP] + k_2K_{eq}'[PP]^2)/(1 + K_{eq}'[PP])$. The conditional constant K_{eq}' ($=K_{eq}/[X]$) obtained in the numerical regression procedure varied with $[Cl^-]$ as required by mechanism 1. Two plausible simple alternative mechanisms were also considered. Both involved a saturation pathway involving attainment of an open conformation of the protein and a nonsaturation pathway involving direct removal of iron from the transferrin. Both mechanisms led to an anion dependence of the microscopic rate and equilibrium constants on $[Cl^-]$ different from that observed experimentally. Furthermore, plots of ln k_1 and ln k_2 vs T^{-1} for mechanism 1 adhere closely to the Arrhenius model, with no curvature or breaks in the plots apparent, as required for true microscopic rate constants, thus arguing further in favor of the correctness of this mechanism.

Introduction

Human serum transferrin is one of a family of iron-binding proteins responsible for transport of iron in the serum and iron sequestering in body fluids, such as milk. It is a single polypeptide chain consisting of 678 amino acid residues arranged into two similar but not identical lobes.[1-5] Each lobe is further organized into two domains, and one Fe(III) ion is bound in the cleft between the two domains along with a (bi)carbonate ion (known as the synergistic anion). The iron-binding ligands have been identified as two tyrosines, a histidine, and an aspartate with the remaining two coordination sites occupied by the synergistic anion, bound in a bidentate manner.[1,2] A number of reviews on the physicochemical behavior of transferrin are available.[3-5]

Considerable interest has focused on the kinetics of iron release from transferrin, both via reduction to weakly bound[6] Fe(II) followed by complexation by a ferrous ion acceptor[7-9] (which provides a significant driving force for the reduction) and by direct chelation of Fe(III). Studies of the latter route using ligands such as acetohydroxamate[10] and *N,N',N''*-tris(5-sulfo-2,3-dihydroxybenzoyl)-1,5,10-triazadecane (3,4-LICAMS)[11] have shown an apparent saturation dependence on chelator concentration of the observed pseudo-first-order rate constants for iron release (k_{obs}) from the two (N- and C-terminal) sites. On the basis of these (as well as iron uptake) results, Bates and co-workers[10] proposed essentially the following mechanism for iron release: (i) A rate-limiting conformational change of the ferric transferrin to an open conformation; (ii) rapid attack of the chelating agent on the iron to form a so-called quarternary complex (since this follows the rate-determining step, it is not detected during iron release

Scheme I[a]

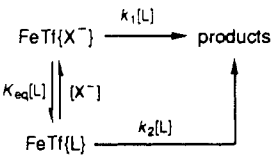

[a] X^- = an anion such as NO_3^-, SO_4^{2-}, or Cl^-; L = an anionic chelating agent, e.g. citrate or PP; $k_1 > k_2$.

* To whom correspondence should be addressed at the Department of Biophysics and Physiology, Albert Einstein College of Medicine, Yeshiva University, 1300 Morris Park Avenue, Bronx, NY 10461.
† Red Cross War Memorial Children's Hospital.
‡ University of Cape Town Medical School.

(1) Bailey, B.; Evans, R. W.; Garrat, R. C.; Gorinsky, B.; Hasnain, S.; Horsburgh, C.; Jhoti, H.; Lindley, P. F.; Mydin, A.; Sarra, R.; Watson, J. L. *Biochemistry* **1988**, *27*, 5804-5812.
(2) Anderson, B. F.; Baker, H. M.; Dodson, E. J.; Norris, G. E.; Rumball, S. V.; Waters, J. M.; Baker, E. N. *Proc. Natl. Acad. Sci. U.S.A.* **1987**, *84*, 1769-1773.
(3) Harris, D. C.; Aisen, P. In *Iron Carriers and Iron Proteins*; Loehr, T. M., Ed.; VCH Publishers: New York, 1989; pp 239-352.
(4) Chasteen, N. D. In *Iron Binding Proteins without Cofactors or Sulfur Clusters*; Thiel, E. C., Eichorn, G. L., Marzilli, L. G., Eds.; Advances in Inorganic Biochemistry Vol. 5; Elsevier: New York, 1983; pp 201-233.
(5) Baldwin, D. A.; Egan, T. J. *S. Afr. J. Sci.* **1987**, *83*, 22-31.
(6) Harris, W. R. *J. Inorg. Biochem.* **1986**, *27*, 41-52.
(7) Ankel, E.; Petering, D. H. *Biochem. Pharmacol.* **1980**, *29*, 1833-1837.
(8) Kojima, N.; Bates, G. W. *J. Biol. Chem.* **1979**, *254*, 8847-8854.
(9) Baldwin, D. A.; Egan, T. J.; Marques, H. M. *Biochim. Biophys. Acta* **1990**, *1038*, 1-9.
(10) Cowart, R. E.; Kojima, N.; Bates, G. W. *J. Biol. Chem.* **1982**, *257*, 7560-7565.
(11) Kretchmar, S. A.; Raymond, K. N. *J. Am. Chem. Soc.* **1986**, *108*, 6212-6218.

0020-1669/92/1331-1994$03.00/0